

Heat and SO₂ Emission Rates at Active Volcanoes – The Case Study of Masaya, Nicaragua

Letizia Spampinato and Giuseppe Salerno
*Istituto Nazionale di Geofisica e Vulcanologia,
Osservatorio Etneo, sezione di Catania, Catania,
Italy*

1. Introduction

The necessity of understanding volcanic phenomena so as to assist hazard assessment and risk management, has led to development of a number of techniques for the tracking of volcanic events so as to support forecasting efforts. Since 1980s scientific community has progressively drifted research and surveillance at active volcanoes by integrated approach. Nowadays, volcano observatories over the world record and integrate real or near-real time data for monitoring and understanding volcano behaviour. Among the geophysical, geochemical, and volcanological parameters, the tracking of temperature changes at several volcanic features (e.g. open-vent systems, eruptive vents, fumaroles) and variations in sulphur dioxide flux and concentration at volcanic plumes are key factors for studying and monitoring active volcanoes.

Temperature is one of the first parameters that have been considered in understanding the nature of volcanoes and their eruptions. Thermal anomalies have proved to be precursors of a number of eruptive events (e.g. Andronico et al., 2005; Dean et al., 2004; Dehn et al., 2002), and once an eruption begins, temperature plays a major role in lava flow emplacement and lava field development (e.g. Ball et al., 2008; Calvari et al., 2010; Lodato et al., 2007). At active volcanoes, temperature has been measured by direct and indirect methodologies (Fig. 1a, c). Direct measurements represent the traditional thermal monitoring carried out at fumaroles, hot springs, molten lava bodies, and crater lakes, using thermocouples (e.g. Aiuppa et al., 2006; Corsaro & Miraglia, 2005). Indirect measurements, also known as thermal remote sensing, can be performed by satellite, ground, and airborne surveys (e.g. Calvari et al., 2006; Spampinato et al., 2011; Wright et al., 2010). Owing to the danger of most kinds of eruption, and the need of monitoring inaccessible areas on volcanoes (e.g. Wright & Pilger, 2008), indirect measurements are especially attractive. Among them, thermal imagery is one of the most widespread and results from the capability to detect the infrared radiation emitted from the surface of hot bodies, and to provide the radiometric map of heat distribution of the body's surface (Spampinato et al., 2011). This has been of primary importance for capturing the evolution of thermal anomalies, which shed light on magma movements at shallow depths (e.g. Calvari et al., 2005). While magma is rising, hot gases

separate from the melt and escape either directly from the main conduits, or indirectly by leaking through fumaroles, fractures, and faults, or by dissolving within crater lakes and hot spring waters, resulting in variations in their temperature and chemical composition. At the surface, these phenomena are also associated with radiative heat fluxes, which can be detected by infrared thermal detectors. The application of thermal imaging to volcanology was largely performed using satellite surveys (e.g. Harris et al., 2011; Vicari et al., 2008), but in the last decade there has been increasing application of compact (hand-held) thermal imagers used from the air or ground (Spampinato et al., 2011).



Fig. 1. Different modes for temperature and volcanic gas sampling. Conventional in situ measurements of (a) the temperature of Hawaiian pāhoehoe lava flow fields (photo by P. Mougini-Mark, volcano.oregonstate.edu), and (b) volcanic gas from the summit fumarole field of Kilauea volcano in 2005. In (c) and (d) ground-based thermal imagery of the Laguna Caliente crater lake (Poás volcano, Costa Rica; 2009) and UV-DOAS measurements of the Santiago crater (Masaya volcano, Nicaragua; 2009) volcanic plume, respectively.

Volcanic degassing plays a key role in magma transport and style, and timing of volcanic eruptions observed at the Earth's surface (e.g. Carroll & Holloway, 1994; Gilbert & Sparks, 1998; Huppert & Woods, 2002; Sparks, 2003). The assessment of volcanic gas composition and flux has become a standard procedure for volcanic monitoring and eruption forecasting, since degassing regimes are fundamentally linked to volcanic processes (e.g. Aiuppa et al., 2007, 2010; Edmonds, 2008; Noguchi & Kamiya, 1963; Oppenheimer, 2003; Sutton et al., 2001). Magma contains dissolved gases that are released into the atmosphere during both quiescent and eruptive degassing phases (e.g. Oppenheimer, 2003). At high pressures, deep beneath the Earth's surface, gases are dissolved in magma; however as soon as magma rises toward the surface, where pressures are lower, gases start to exsolve according to the solubility-pressure relationship of each species, as well as compositional and diffusional

constraints (e.g. Carroll & Holloway, 1994; Carroll & Webster, 1994; Oppenheimer, 2003; Spilliaert et al., 2006; Villemant & Boudon, 1999). The abundance and final gas phase composition of the emitted plume depends on magma composition(s), volatile fugacities, crystallisation, and on the dynamics of magma degassing, including kinetic effects (e.g. Giggenbach, 1996; Oppenheimer, 2003; Symonds et al., 1994, 2011). However, at the surface, the composition and flux of volcanic gases may change with time, reflecting variations in the magmatic feeding system of the volcano. Hence, by studying and tracking this variability a number of parameters, such as magma residing depths and the amount of degassing magma bodies can be determined (Allard, 1997; Steffke et al., 2010).

Among the volcanic gas species, sulphur dioxide (SO₂) is one of the most well investigated in remote sensing (e.g. Bluth et al., 2007; Carn et al., 2003; Galle et al., 2010; Hamilton et al., 1978; McGonigle et al., 2009; Salerno et al., 2009a; Williams-Jones et al., 2008; Sweeney et al., 2008; Thomas & Watson, 2010). As for temperature, SO₂ concentration and emission rates can be measured using both direct sampling and non-contact remote sensing techniques (Fig. 1b, d; e.g. Finnegan et al., 1989; Giggenbach & Goguel, 1989; McGee & Sutton, 1994; McGonigle & Oppenheimer, 2003; Mougini-Mark et al., 2000). The latter carried out during air- and ground-based surveys and on satellite platforms, are based on optical spectroscopy. Since the 1970s, SO₂ flux has been remotely measured using the CORrelation SPECTrometer (COSPEC; Newcomb & Millán, 1970; Stoiber & Jepsen, 1973; Stoiber et al., 1983) at several volcanoes worldwide (e.g. Caltabiano et al., 1994; Malinconico, 1979; Realmuto, 2000; Sutton et al., 2001; Williams-Jones et al., 2008). Over the last 10 years the advent of small, commercial and low cost spectrometers (Mini-DOAS, Galle et al., 2003; RMDI, Wardell et al., 2003; MUSE, Rodriguez et al., 2004; Flyspec, Horton et al., 2006; Dual-Field of View, McGonigle et al., 2009) offered a valuable replacement to the outdated COSPEC. In particular, the combination of Ultraviolet (UV) spectrometers with the Differential Optical Absorption Spectroscopy (DOAS) analytical method (Noxon, 1975; Platt, 1994; Platt & Stutz, 2008) improved significantly data collection, offering a number of advantages such as the possibility of obtaining measurements in the challenging environments typical of volcanic areas, detection of other plume species (Bobrowski et al., 2003; O'Dwyer et al., 2003; Oppenheimer et al., 2005), and collection of high-resolution SO₂ flux by permanent scanner networks (e.g. Arellano et al., 2008; Edmonds et al., 2003; Salerno et al., 2009a, 2009b).

Our intent here is to discuss findings and implications arising from the integration of thermal imaging-derived temperature and SO₂ emission rates by UV-DOAS spectroscopy collected in March 2009 at Masaya volcano, Nicaragua. Calibrated temperatures from thermal imagery can provide qualitative as well as quantitative information, fundamental insights and parameters contributing to understanding and modelling of several eruptive features. Anomalies in SO₂ emission rates have been often documented at several volcanoes prior to eruptive crisis (e.g. Casadevall et al., 1981; Daag et al., 1996; Kyle et al., 1994; Malinconico, 1979; Sutton et al., 2001; Williams-Jones et al., 2008; Young et al., 1998; Zapata et al., 1997). In syn-eruptive stages, anomalies in the SO₂ flux pattern might indicate variations in the eruptive style and regime associated with changes in the volcano shallow feeder system (e.g. Andronico et al., 2005; Delgado-Granados et al., 2001; Olmos et al., 2007; Spampinato et al., 2008a; Spilliaert et al., 2006). At open-vent systems, in non-eruptive phases, changes in SO₂ flux emission have provided information on increases or decreases

of magma supply in the shallow plumbing system (Allard, 1997; Wallace & Gerlach, 1994) suggesting likely volcanic unrests or magma migration towards peripheral areas of the volcano edifice, respectively.

There is still much to explore about volcano behaviour and eruptive mechanisms, however, the combination of different types of monitoring techniques is crucial for constraining baselines for predicting phases of volcano unrests and for gaining useful insights for volcano hazard assessment.

2. Masaya volcano

Masaya is an open-vent, basaltic shield volcano (560 m a.s.l.) sited in western Nicaragua (Central America). The volcano edifice includes a 11×6 km-elongated caldera that formed ~2,500 yrs ago as a result of a 8 km^3 -basaltic ignimbrite eruption (Williams, 1983). The caldera hosts a complex of lavas and cinder cones, with cones cut by pit craters, of which the Santiago is the presently active (e.g. Harris, 2009; Roche et al., 2001; **Fig. 2**). Over time, the Santiago pit crater has been characterised by the development of ephemeral lava lakes

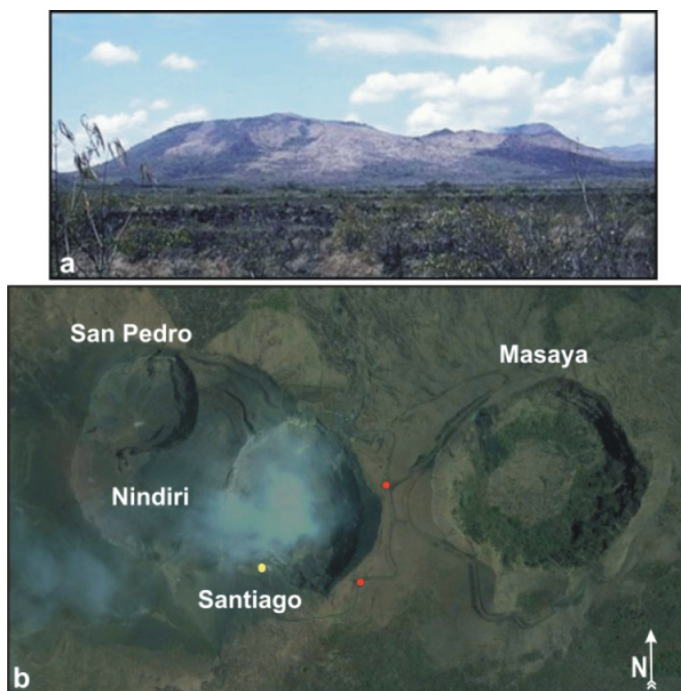


Fig. 2. (a) Photograph of Masaya volcano taken from NNE (geoalba.com). (b) Satellite image of Masaya volcano summit area (googleEarth 2011). San Pedro, Nindiri, Santiago, and Masaya craters are shown (see Harris, 2009 for more details). The Santiago crater is the currently active and the site of our investigation. The yellow and red dots indicate the sites from which thermal imagery and SO_2 amount measurements were respectively carried out in March 2009.

(Allen et al., 2002), explosive activity (e.g. Duffell et al., 2003; Perez et al., 2009; Rausch & Schmincke, 2010) effusive eruptions (e.g. Harris, 2009), intense degassing (e.g. Branan et al., 2008; Kern et al., 2009a; Williams-Jones, 2001), and phases of inner crater collapses (e.g. McBirney, 1956; Harris, 2009; Rymer, et al., 1998). The volcano activity has consisted of phases of quiescent degassing for over 150 years, punctuated by intermittent gas crises associated with high SO₂ emissions (e.g. Delmelle et al., 2002; Stix, 2007), and minor explosive phases throwing ejecta around the summit area, of which the most significant event of the last 30 years occurred in 2001 (e.g. Branan et al., 2008; Duffell et al., 2003).

The persistent loose of gas has been interpreted as the result of periodic magma convective overturn within the volcano shallow feeding system (Delmelle et al., 1999; Horrocks, 2001; Horrocks et al., 1999). It has been estimated that during the last 150 years, degassing has been supplied by ~10 km³ of magma (e.g. Rymer et al., 1998; Stoiber et al., 1986).

The easy accessibility of Masaya summit area has made the volcano an ideal natural laboratory, where a number of different monitoring techniques, direct and indirect observations, have been carried out since the onset of the post-1993 degassing crisis (e.g. Allen et al., 2002; Galle et al., 2003; Mather et al., 2003; Martin et al., 2009; Nadeau & Williams-Jones, 2009). Tracking of Masaya's activity has been of primary importance not only for the understanding and modelling of the volcano deep processes (e.g. Stix, 2007; Williams-Jones et al., 2003), but also for the potential health hazard posed by the volcanic gas emissions (Delmelle et al., 2002). In fact, due to the low altitude of the volcano edifice, the continuous degassing from the Santiago crater represents a threat for people living close to the volcano foot (**Fig. 3**).

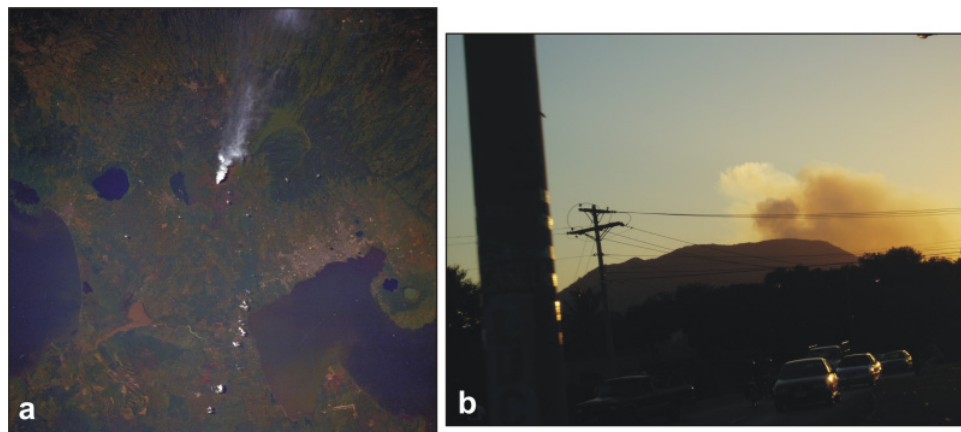


Fig. 3. (a) Satellite image showing the persistent volcanic plume from Santiago crater (zonu.com). (b) Photograph of Masaya volcano and its volcanic plume taken in March 2009 from ENE.

The persistent degassing from Santiago crater has been extensively studied by remote sensing methodologies, spanning from infrared to ultraviolet spectroscopy, carried out during ground-based surveys or by satellite platforms (e.g. Branan et al., 2008; Burton et al., 2000; Horrocks et al., 2003; Martin et al., 2010; Nadeau & Williams-Jones, 2009; Thomas &

Watson, 2010). Here we report on the Santiago's crater activity that we observed, between 20 and 24 March 2009, carrying out simultaneous volcanic plume measurements using a portable infrared imager and an ultraviolet spectrometer.

3. Infrared and ultraviolet remote sensing

Following we shortly report the main techniques for the acquisition of thermal imagery and SO₂ fluxes and amounts, and the instrumental specifications and details on the methodology of data collection during the March 2009 field campaign at Masaya volcano.

3.1 Thermal imagery

During the 20–24 March 2009, we recorded thermal imagery of the Santiago crater using a P25 FLIR (Forward Looking InfraRed Systems) portable thermal camera from the Sapper car park on the south-western crater rim. The instrument is an uncooled microbolometer with a 320 × 240 pixel array sensitive to the 7.5–13 μm wave band with a 24 × 18° field-of-view (FOV). Its quoted precision is ±2% and the thermal sensitivity is less than 273.23 K at 303.15 K. The camera is equipped with three dynamic temperature ranges 233.15 to 393.15 K, 273.15 to 773.15 K, and 623.15 to 1773.15 K, of which we used the middle one. In order to make a first-order correction for the atmospheric effects (e.g. Spampinato et al., 2011), we input in the camera internal software the measured line-of-sight from the crater bottom (~340 m; see yellow dot in Fig. 2 for the camera site), and the daily mean temperature and relative humidity of the air (306.15 K and 38% on 20 March; 306.15 K and 32% on 21 March; 303.15 K and 40% on 22 March; 303.15 K and 42% on 23 March; and 306.15 K and 35% on 24 March). Considering the camera instrumental specifications and the path length of ~340 m, the nominal pixel size was of ~0.47 m. According to Branan et al. (2008), we used an emissivity (ε) value of the hot source of 1, and given that emissivity has non-Lambertian behaviour, we measured the inclination angle of the camera (70°) for error evaluation (e.g. Ball and Pinkerton, 2006; Spampinato et al., 2011). Images were collected every 8 seconds between 17:06:27 and 18:48:29 (here after all times are in GMT) on 20 March, 20:10:47 and 21:40:45 on 21 March, 15:53:04 and 18:22:54 on 22 March, 16:05:26 and 18:31:47 on 23 March, and 15:39:02 and 17:07:34 on 24 March. Along the five days of the survey, thermal imagery was recorded from the same identical position and viewing inclination (Fig. 2).

A recent account on the uncertainty in thermal imagery-derived data was provided by Spampinato et al. (2011).

3.2 UV spectroscopy

On 20, 21, 23 and 24 March 2009, we carried out SO₂ flux measurements (tonnes day⁻¹) by car-based traverses along the Llano Pacaya road (15 km downwind of the Santiago crater, see Martin et al., 2010) and along the Ticuantepe road (5 km downwind of the Santiago crater, see Martin et al., 2010). Optimal integration time for the collection of spectra in the traverse technique was 100 ms, and 50 spectra were co-added to improve the signal-to-noise ratio. Spectra were time- and position-stamped using a USB GPS receiver. In addition, between 20, 21, 22, and 23 March, we collected also SO₂ column amounts (CA, in ppm × m) using a UV spectrometer and scattered sunlight as the light source. Individual spectra were

recorded from fixed position from the eastern flank of the Santiago crater, ~400 m far from the plume (see **Fig. 2** for the measurement sites) at sampling rate between 14 and 17 s.

For both kinds of measurement techniques, we used an Ocean Optics USB2000 spectrometer. The instrument comprises a 2048 pixel-detector-array and diffraction grating with 3600 grooves per mm, which combined with a 200 μm entrance slit, delivers a spectral resolution of ~0.44 nm FWHM in the 295-375 nm wavelength range. To perform SO₂ flux traverses the instrument was mounted inside a car and connected via fibre optic cable to a telescope (8 mrad FOV) oriented vertically upwards.

SO₂ CA were retrieved using the WinDoas software package (Fayt & van Roozendaal, 2001) applying the standard DOAS method (Platt & Stutz, 2008). The ring spectrum (e.g. Fish & Jones, 1995; Solomon et al., 1987) was calculated from the clear sky-spectrum (spectrum collected out of the plume) following the approach of Chance (1998). Both laboratory spectra of SO₂ and O₃ (Malicet et al., 1995; Vandaele et al., 1994) and the Ring spectrum were convolved to the spectrometer's resolution. UV spectra were evaluated in the 305-316 nm window to yield the time-series of the SO₂ CA in the FOV of the spectrometer. SO₂ flux was evaluated following Stoiber et al. (1983). Wind speed was measured every 10 minutes using a portable hand-held anemometer. In the days of our observations, mean wind speed and direction were of ~5 m s⁻¹ toward the SW. Error in SO₂ flux detection by UV spectroscopy depends mainly on the uncertainty in the plume-wind speed (e.g. Doukas, 2002; Mather et al., 2006). Stoiber et al. (1983) estimated uncertainty in flux calculation between 10-40%. Negligible uncertainty arises from the error in the retrieved SO₂ CA (e.g. Kern, 2009; Platt & Stutz, 2008), multiple scattering (e.g. Kern et al., 2009b; Millan, 1980), the presence of volcanic ash in the plume (Andres & Schimd, 2001), or SO₂ depletion (McGonigle et al., 2004; Nadeau and Williams-Jones, 2009; Oppenheimer et al., 1998). During our campaign, the plume always appeared to be bright and free from ash and situated below the clouds, thus we can consider the influence of multiple scattering and ash to be negligible.

4. Observations of the Santiago crater activity

Along the 5 day-observation period, the Santiago activity consisted of persistent degassing from two vents opened at the crater floor (Martin et al., 2010; Vent 1 and Vent 2 in **Fig. 4**). From the Santiago crater SW rim, from which we carried out thermal imagery (**Fig. 2**), Vent 2 was clearly visible at the naked eye, whereas Vent 1 was hidden by Vent 1 plume, and thus recognisable only by infrared optics (**Fig. 4c**). Thermal imagery showed that Vent 2 was eventually wider than Vent 1 (**Fig. 4c**). Applying an apparent temperature threshold of 300 K on thermal images and considering the nominal pixel size of ~0.47 m, we estimated an area of ~450 and ~715 m² for Vent 1 and Vent 2, respectively. Owing to the oblique imagery, we consider such areas as minimum estimates.

The two vents were both persistently degassing with the two plumes joining together a few seconds after the emission (**Fig. 4b**). Qualitatively, the plume seemed to be whitish and denser next to the crater floor (**Fig. 4b**) and transparent and more diluted close to crater rim (**Fig. 4a**). Plume conditions varied also according to the time of day, i.e. more transparent in the morning and more condensed in the evening (Burton et al., 2001; Martin et al., 2010; Mather et al., 2003). Along the 5-day-survey, we did not detect any explosion; however thermal images showed that the quiescent degassing observed at the crater exit, had in reality a pulsating behaviour at the vent region (**Fig. 5**).

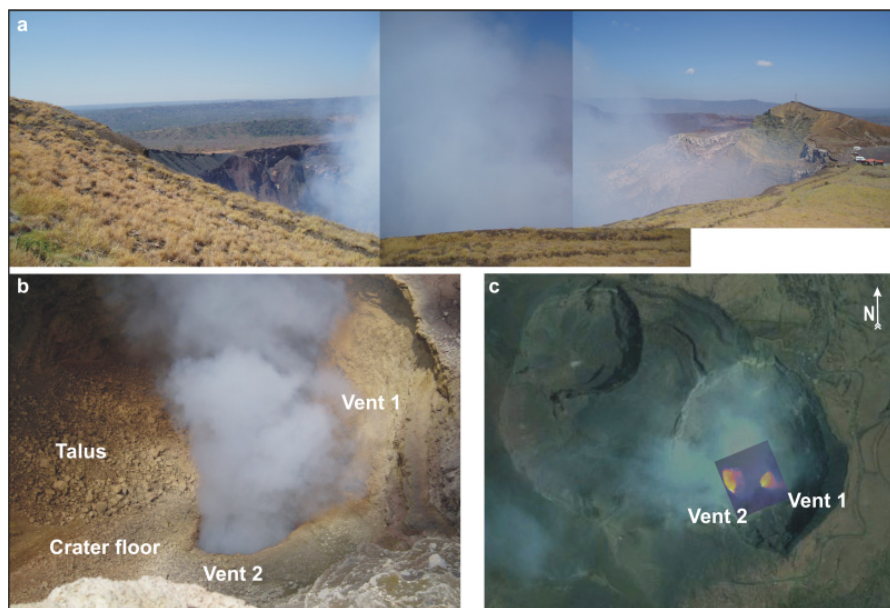


Fig. 4. (a) Photograph of the Santiago crater rim and its volcanic plume taken from the SSE rim on 22 March 2009. (b) Photograph of the two degassing vents opened at the Santiago crater floor taken from the SW rim on 22 March 2009. (c) Zoom of the satellite image of Masaya volcano summit area (googleEarth 2011) shown in Fig. 2. The overlapped thermal image localises the position of Vent 1 and Vent 2 within the Santiago crater. The thermal image was recorded on 22 March 2009 from the SW crater rim.

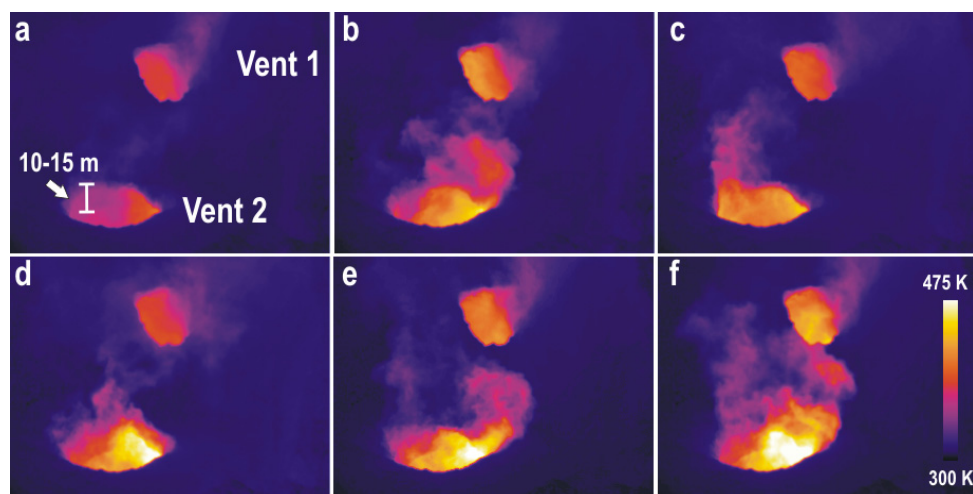


Fig. 5. (a-f) Thermal image sequence showing the degassing pulsating behaviour at both vents. The sequence was recorded on 21 March 2009 from the Santiago crater SW rim.

In addition, thermal images revealed that the magma level inside the two vents remained below both vent rims allowing estimation of the crusted crater floor thickness; that was of ~10-15 m (Fig. 5). Next to the degassing vents, the crater floor was characterised by talus coverage due to the collapses of the eastern crater inner walls (Fig. 4b).

5. Results and discussion

Following we report results of the analysis of thermal image and SO₂ CA and flux data, providing interpretation of the relationship between temperature pattern and heat flux, and SO₂ concentration and emission rates.

5.1 Thermal imaging-derived data

In figure 6, we have plotted the variability of the maximum and mean apparent temperatures (K) of Vent 1 (Fig. 6a, b, d, f, and h) and Vent 2 (Fig. 6c, e, g, and i) over time, along the five days of measurements (of which we lack Vent 2 imagery of the first day). Overall, Vent 2 plume showed somewhat higher temperatures than those of Vent 1 with peak values of ~500 K and maximum means of ~400 K, with respect to the ~460 K and ~380 K of Vent 1. However, the temperature difference between the two vents might have resulted from the viewing angle difference with which the two vents were imaged (Fig. 5).

In detail, Vent 1 maximum temperatures varied between 360-454 K on 20 March, 374-475 K on 21 March, 372-453 K on 22 March, 355-466 K on 23 March, and between 376-452 K on 24 March (Fig. 6a, b, d, f, and h). The vent mean values ranged between 338-384 K, 346-388 K, 344-384 K, 336-392 K, and 348-386 K, from 20 to 24 March, respectively (Fig. 6a, b, d, f, and h). Vent 2 maximum temperatures fluctuated between 385-510 K, 363-488 K, 376-500 K, and 373-504 K on 21, 22, 23, and 24 March, respectively (Fig. 6c, e, g, and i). Mean temperatures of Vent 2 varied between 343-405 K, 332-394 K, 340-397 K, and 336-396 K from 21 to 24 March, respectively (Fig. 6c, e, g, and i). Both the maximum and mean temperature trends of the two vents are characterised by the overlapping of waveforms of different amplitudes that we consider in section 5.3.

Using the estimated areas of 450 and 715 m² respectively for Vent 1 and Vent 2, $\epsilon = 1$, and the most representative thermal images (i.e. those with the highest mean temperature values and the lowest standard deviations; e.g. Spampinato et al., 2008b), we have calculated magma heat loss by radiation (Q_{rad} ; MW) from the two vents between 20 and 24 March 2009 (Fig. 7).

Figure 7 shows the variability of the daily mean Q_{rad} of the two vents (Vent 1 grey line and Vent 2 black line). As previously argued, given that the areas considered are minimum values, the Q_{rad} estimates in figure 7 correspond to minimum daily mean values. Along the days of observation, the total Q_{rad} from the two vents remained quite stable varying between 1.2 and 1.8 MW.

Note that we have considered only the radiated flux as we have assumed that the incidence of heat loss by conduction (Q_{cond}) and convection (Q_{conv}) was reduced. In particular, at Santiago crater, Q_{cond} implies heat dissipation from the walls of the conduit; however, following Giberti et al. (1992), we have assumed that after years of persistent activity the volcano shallow system is likely long-established and well insulated. Thus, we have

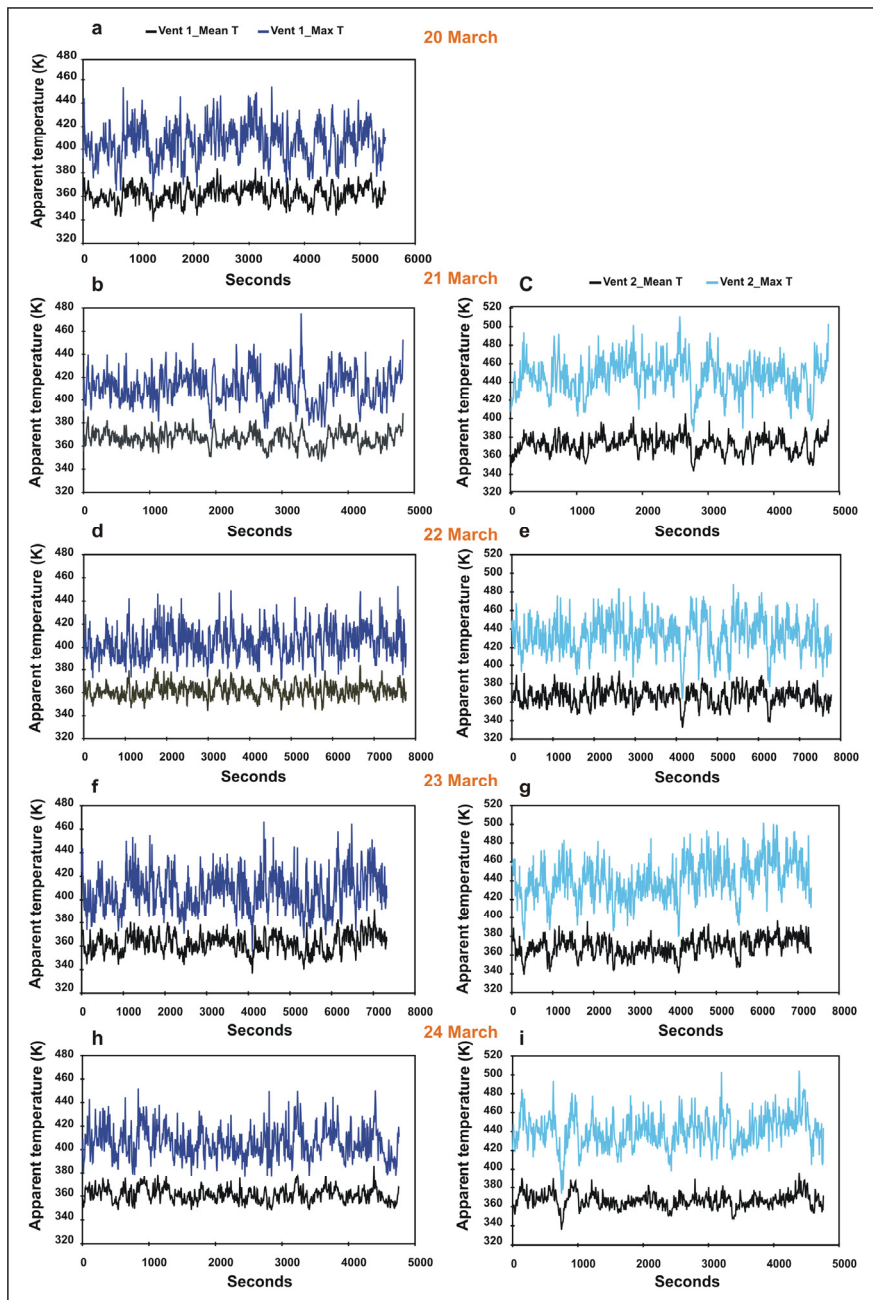


Fig. 6. Temporal variability of Vent 1 (on the left; a, b, d, f, and h) and Vent 2 (on the right; c, e, g, and i) maximum and mean apparent temperatures during the 20-24 March 2009 ground-based thermal surveys.

supposed that conduction to the country rock was irrelevant with respect to Q_{rad} . At the same manner, we have neglected the contribution of Q_{conv} . In fact, during the 5-day survey, wind conditions were quite stable ($\sim 5 \text{ m s}^{-1}$; free convection, e.g. Keszthelyi & Denlinger, 1996; Keszthelyi et al., 2003; Neri, 1989), and the magma level was confined at least $\sim 15 \text{ m}$ below the crater floor (Fig. 5). Hence, magma surface was not directly exposed to wind action.

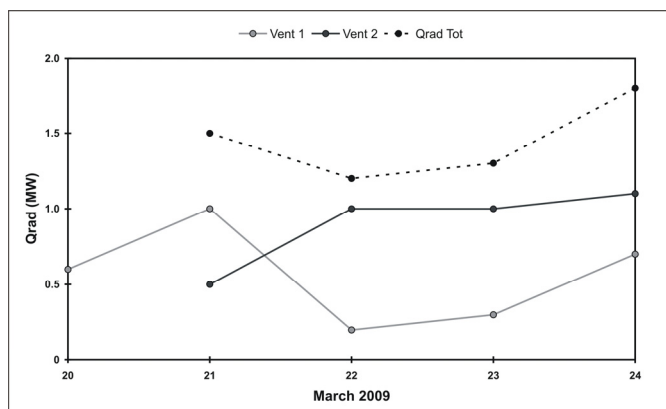


Fig. 7. Variability of Vent 1 and Vent 2 radiant heat flux from 20 to 24 March 2009. The grey line refers to Vent 1, the black line to Vent 2, and the black-dotted line to the total heat flux radiated by the two vents.

5.2 SO₂ column amounts and fluxes

Figure 8 reports the SO₂ CA collected between 20 and 23 March 2009 at the Santiago crater volcanic plume (a, b, c, and d). Given that measurements were taken out of the crater (Fig. 2), the amounts represent the contribution of both vents.

The highest SO₂ concentrations were detected on 20 March when the maximum CA was $5430 \text{ ppm} \times \text{m}$ (mean of $1832 \text{ ppm} \times \text{m}$; Fig. 8a), with respect to the maxima of 2185, 2672, and $2590 \text{ ppm} \times \text{m}$ (means of 472, 966, and $885 \text{ ppm} \times \text{m}$) recorded on 21, 22, and 23 March, respectively (Fig. 8b, c, d). As for the temperature data sets of figure 6, the SO₂ CA time-series show several high amplitude fluctuations on which higher frequency components are superimposed. In particular, on the 20 March time-series we recognised at least four main fluctuations peaking at 5430 (17:34:36), 5360 (17:56:01), 5240 (18:07:03), and $4800 \text{ ppm} \times \text{m}$ (18:21:52). In terms of maximum SO₂ concentrations, the fluctuations are characterised by a decreasing trend (Fig. 8a). On 21 March, we observed a more defined trend in which we clearly recognise three fluctuations of the SO₂ CA with maximum values of 1998 (20:42:51), 2186 (21:05:17), and 1583 (21:25:03) $\text{ppm} \times \text{m}$ (Fig. 8b). In the 22 March time-series, we distinguished four main fluctuations (Fig. 8c) with maximum SO₂ CA of 2058 (15:41:08), 2672 (16:26:04), 1794 (17:12:57), and 1942 $\text{ppm} \times \text{m}$ (17:43:51). Note that due to the length of the time-series, we could not determine the exact end of the last fluctuation (Fig. 8c). The last time-series, recorded on 23 March, displays four main SO₂ CA fluctuations with peaks of 2088 (16:42:43), 2257 (17:03:13), 2104 (17:40:54), and $2590 \text{ ppm} \times \text{m}$ (18:04:16), respectively (Fig. 8d). As for the maximum and mean temperature trends of figure 6, the nature of the overlapped waveforms, recognised in figure 8, are investigated in section 5.3.

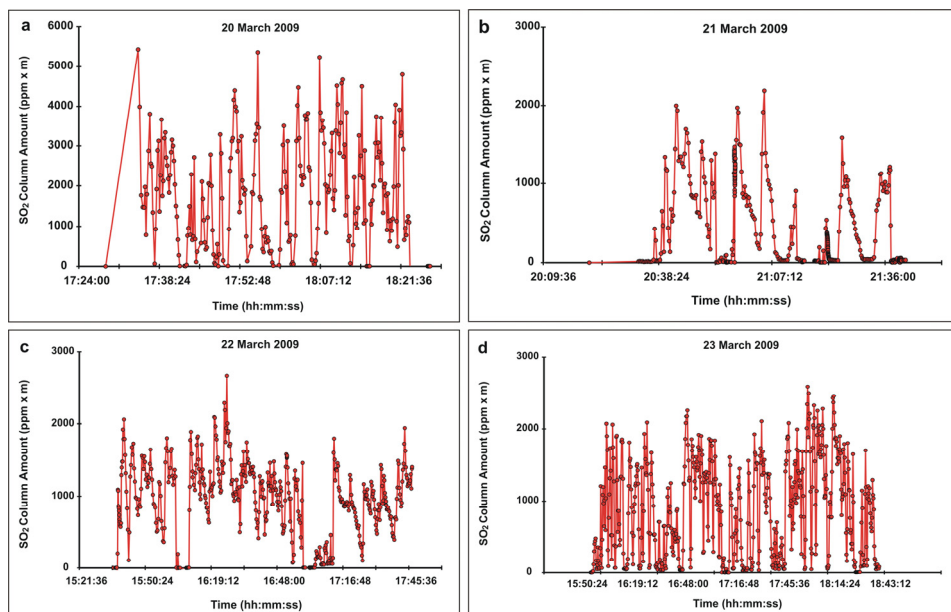


Fig. 8. Temporal variability of SO₂ CA from Vent 1 and Vent 2 between 20 and 23 March 2009. The CA were collected from fixed position and from different sites (see Fig. 2b for details).

During the March 2009 field campaign, we measured also the SO₂ flux by car-based traverses (Fig. 9; see also Martin et al., 2010). In detail, we carried out three traverses on 20 March (from 20:20:00 to 21:30:00), six on the 21st (from 16:40:00 to 18:30:00), four on the 23rd (from 20:30:00 to 22:10:00), and ten on 24 March (from 15:15:00 to 16:50:00).

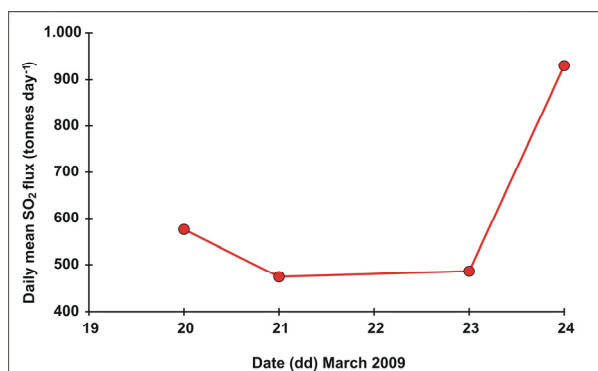


Fig. 9. Daily mean SO₂ flux measured during the 20, 21, 23, and 24 March 2009 by car-based traverses.

Overall, the daily mean SO₂ flux was characterised by an increasing trend from 20 to 24 March, when the flux reached values of 1350 and 1325 tonnes day⁻¹ (Fig. 9). Daily mean

fluxes (± 1 standard deviation) were 580 ± 180 (20 March), 470 ± 100 (21 March), 490 ± 170 (23 March), and 930 ± 280 tonnes day⁻¹ (24 March). The average SO₂ flux measured during the 4-day survey was of 690 tonnes day⁻¹ (Martin et al., 2010).

5.3 Comparative signal processing and results

Figure 10 shows the behaviour of the mean apparent temperatures of Vent 1 and Vent 2 with respect to the pattern of the SO₂ CA from 20 to 23 March 2009. In order to make a reasonable comparison between temperatures and SO₂ CA, we have plotted the 10-point running means of both parameters. The black and grey lines refer to Vent 1 and Vent 2 mean temperatures, respectively, and the red line to the SO₂ CA. In addition, moving average has allowed us to filter the very high frequency signals, which are commonly related to noise effects of variable nature such as turbulence of the volcanic plume next to the vent area and drifting of the plume within the FOV of the UV spectroscopy system.

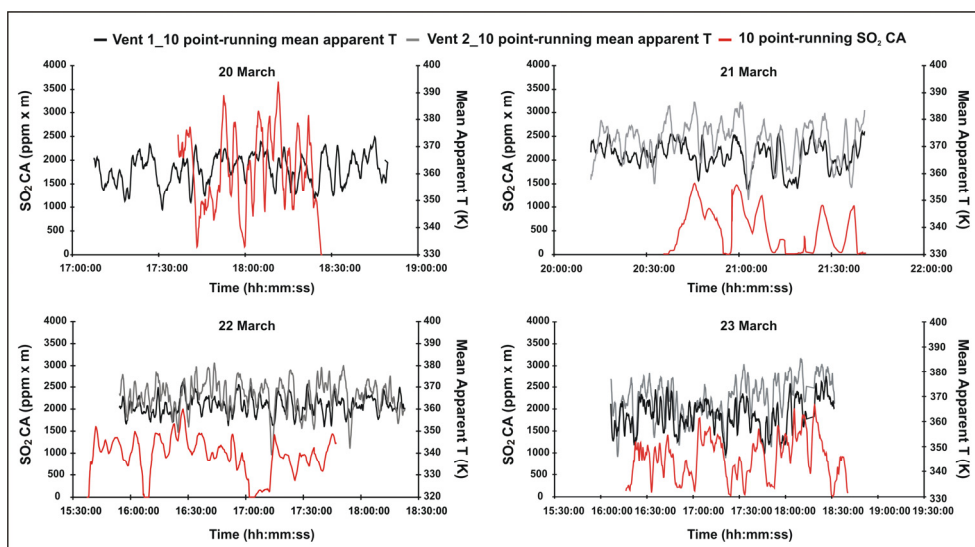


Fig. 10. Comparison between the temporal trends of Vent 1 and Vent 2-10 point running mean apparent temperatures and the 10-point running mean of the SO₂ CA.

Along the four days of measurements, temperatures and SO₂ CA are well correlated, though they show a somewhat shifting due to the different sites from which temperatures and CA were measured, i.e. the thermal camera pointed directly at the vents whereas SO₂ concentrations were taken out of the Santiago's crater rim (Fig. 2). Both temperatures and CA are characterised by superimposed cycles of different periods (Fig. 10). In order to investigate the reliability of the qualitatively observed cycles, we have carried out time-series analysis by Fast Fourier transform on both mean apparent temperatures and SO₂ CA (Fig. 11). Figure 11 shows the power spectra and the statistical significance calculated considering the hypothesis of a background red noise, and thus we have considered reliable only the peaks lying above the green line, which represents the 95% confidence spectrum (e.g. Spampinato et al., 2008b; Torrence & Compo, 1998).

Vent 1 shows significant periods of 1-2 min and 8 min on 20 March, 1-3 min and 15 min on 21 March, 1-3 min, 5 min, 7 min, and 13 min on 22 March, 2 min, 4 min, and 46 min on 23 March, and of 1 min, 6 min, 11 min, and 18 min on 24 March (Fig. 11). Vent 2 is characterised by significant peaks of 1 min and 7 min on 21 March, 1-3 min, 7 min, and 21 min on 22 March, 1 min, 7 min, and 28 min on 23 March, and of 1 min, 7 min, and 15 min on 24 March (Fig. 11). The SO₂ CA time-series display major peaks at 1-2 min and 4 min on the 20th, 2-3 min, 4-5 min, 7 min, and 10 min on the 21st, 1-3 min, 5 min, 8 min, and 11 min on the 22nd, and at 1-3 min and 4 min on 23 March (Fig. 11).

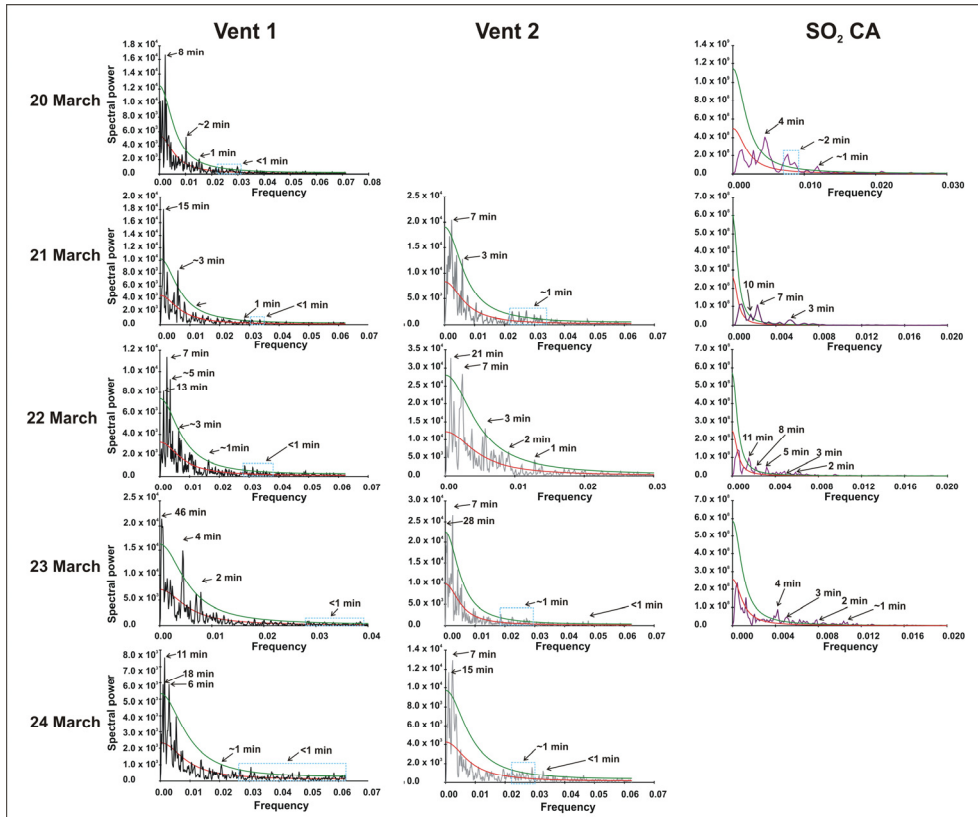


Fig. 11. Power spectra and statistical significance of Vent 1 and Vent 2 mean temperature time-series and of the SO₂ CA data sets collected between 20 and 24 March 2009. The green and red lines represent the 95% and 75% confidence spectra, respectively. In the figure, we have reported only the period of peaks above the green lines. The cyan dashed rectangles enclose low spectral power peaks with periods below 1 minute.

Observing in details the power spectrum time-series of figure 11, we detected also peaks that, though they do not overcome the green line, they are above the red lines representing the 75% confidence spectra. Most of these peaks consist of low frequency signals, between ~40 and 50 min in the temperature time-series and ~30 and 50 min in the SO₂

concentrations, which due to the reduced length of the data sets have a low spectral power (Fig. 11).

5.4 Data interpretation and concluding remarks

Here we have reported on the integration of thermal imaging-derived data with both SO₂ fluxes and concentrations from the Santiago active crater of Masaya volcano in March 2009. As already reported by Martin et al. (2010), in that period the crater activity was fed by two vents opened at the crater floor. The opening and closure of vents over time (e.g. Branan et al., 2008), combined with results from structural and geophysical studies (Rymer et al., 1998; Williams-Jones et al., 2003), has suggested that the vents result from the collapses of the thin crusted roof of the volcano shallow magma accumulation zone (Martin et al., 2010). Thermal imagery collected during our campaign allowed us to infer that the magma surface within the two vents was at least ~10-15 m below the surface (Fig. 5a; Martin et al., 2010), suggestive of drop of the magma level over time. Magma level fluctuations have been commonly detected at several basaltic volcanoes (e.g. Stromboli, Calvari et al., 2005; Kilauea, Tilling, 1987). In particular at lava lakes such as Erta 'Ale volcano in Ethiopia, variations in magma level within the crater have been related to magma pressures in the connected reservoir (Oppenheimer & Francis, 1997), thus to changes in the magma supply rate (e.g. Oppenheimer et al., 2004; Spampinato et al., 2008b).

Although Masaya is currently at minimum in its degassing cycle (Williams-Jones et al., 2003), during the time of our observations, the eruptive activity consisted of steady intense degassing from the two vents (the total volatile flux was of 14,000 tonnes day⁻¹; Martin et al., 2010). Except for the first day of survey, SO₂ CA recorded between 21 and 23 March were in agreement with those previously observed by Branan et al. (2008), marking the overall stable state of the volcano activity over long time-scales (Martin et al., 2010).

Peaks in brightness temperature of Vent 2, where somewhat higher with respect to Vent 1 (Fig. 6), likely due to vent geometry combined with the oblique imagery. However, they are comparable with temperatures recorded by Branan et al. (2008) in February 2002 and March 2003 using a thermal infrared thermometer. Whilst maximum apparent temperatures showed greater variability, mean apparent temperatures of both vents ranged between ~340 and 380 K, thus marking the quite stable background of the degassing mode.

The minimum total radiant heat power outputs estimated for the two vents did not display any remarkable variation as well, ranging from ~1.2 to 1.8 MW. The increasing trend of the radiant heat power output from 20 to 24 March can be found also in the pattern of the daily mean SO₂ fluxes, whose values pass from ~460 to 1350 tonnes day⁻¹. This suggests that, during our campaign the day-to-day variability of mean SO₂ flux might not be largely affected by wind speed uncertainty (Martin et al., 2010), as thermal imagery and SO₂ traverses were carried out from different sites and with different geometrical viewing, i.e. pointing directly the vents and crossing the plume from below. The simultaneous variations of both fluxes suggested to us that within the long-term degassing cycles (on the scale of years) of Masaya (Williams-Jones et al., 2003), there might be shorter-term sub-cycles (on the order of days) related to processes occurring within the volcano shallow feeding system (Martin et al., 2010; Nadeau & Williams-Jones, 2009; Witt et al., 2008). In detail, we believe that the increase in heat and SO₂ release might be connected to the rising of a new hot and

gas-rich batch of magma from the volcano shallow reservoir feeding the persistent degassing of this volcano, through processes of magma overturning (Harris et al., 1999; Martin et al., 2010).

Figure 10 shows that both the thermal and SO₂ column amount time-series are not only correlated but they are both characterised by high and low frequency cycles, of which we have recognised periodicities on the order of minutes, of tens of minutes, and wider fluctuations of almost a hour. Owing to instrumental limitations, we could not record frequencies of tens of seconds associated with gas puffing characteristic of Santiago's degassing (Branan et al., 2008; Williams-Jones et al., 2003). Combining our observations with previous interpretations of lava lake dynamics and models (e.g. Spampinato et al., 2008b; Witham et al., 2006), we propose that cycles on the scale of minutes might relate to rates of gas bubbles/trains of bubbles bursting at the magma surface. Instead longer fluctuations in both thermal and SO₂ concentration trends might result from gradual variations in gas supply rate. However longer time-series are needed in order to better understand the meaning of these degassing cycles, especially those referring to the long fluctuations. In a site like Masaya volcano representing the ideal natural laboratory, the install of multi-parametric permanent stations will open up opportunities of long-term observations of the volcanic activity allowing refinement of models developed for open-vent volcanic systems.

6. Acknowledgements

LS and GGS thank C. Oppenheimer, GM Sawyer and RS Martin for sharing fieldwork and ideas. The field campaign in Nicaragua was part of the research project 'Understanding volcanic degassing, magma dynamics at persistently degassing basaltic volcanoes: a novel approach to linking volcanic gases and magmatic volatiles within a physical model'. University of Cambridge-University of Bristol-Natural Environment Research Council (NERC).

7. References

- Aiuppa, A., Federico, C., Giudice, G., Gurrieri, S. & Valenza, M. (2006). Hydrothermal buffering of the SO₂/H₂S ratio in volcanic gases: Evidence from La Fossa Crater fumarolic field, Vulcano Island. *Geophys. Res. Lett.*, 33, L21315, doi:10.1029/2006GL027730.
- Aiuppa, A., Moretti, R., Federico, C., Giudice, G., Gurrieri, S., Liuzzo, M., Papale, P., Shinohara, H. & Valenza, M. (2007). Forecasting Etna eruptions by real-time observation of volcanic gas composition. *Geology*, 35(12), pp. 1115-1118.
- Aiuppa, A., Cannata, A., Cannavò, F., Di Grazia, G., Ferruccio, F., Giudice, G., Gurrieri, S., Liuzzo, M., Mattia, M., Montalto, P., Patane, D. & Puglisi, G. (2010). Patterns in the recent 2007–2008 activity of Mount Etna volcano investigated by integrated geophysical and geochemical observations. *Geochim. Geophys. Geosyst.*, 11, Q09008, doi:10.1029/2010GC003168.
- Allard, P. (1997). Endogenous magma degassing and storage at Mount Etna. *Geophys. Res. Lett.*, 24(17), pp. 2219-2222.

- Allen, A.G., Oppenheimer, C., Ferm, M., Baxter, P.J., Horrocks, L.A., Galle, B., McGonigle, A.J.S. & Duffell, H.J. (2002). Primary sulphate aerosol and associated emissions from Masaya volcano, Nicaragua. *J. Geophys. Res.*, 107(D23), 4682.
- Andres, R.J. & Schimid, J.W. (2001). The effects of volcanic ash on COSPEC measurements. *J. Volcanol. Geotherm. Res.*, 108, pp. 237-244.
- Andronico, D., Branca, S., Calvari, S., Burton, M.R., Caltabiano, T., Corsaro, R.A., Del Carlo, P., Garfi, G., Lodato, L., Miraglia, L., Muré, F., Neri, M., Pecora, E., Pompilio, M., Salerno, G. & Spampinato, L. (2005). A multi-disciplinary study of the 2002-03 Etna eruption: Insights into a complex plumbing system. *Bull. Volcanol.*, 67, pp. 314-330.
- Arellano, S.R., Hall, M., Samaniego, P., Le Pennec, J.-L., Ruiz, A., Molina, I. & Yepes, H. (2008). Degassing patterns of Tungurahua volcano (Ecuador) during the 1999-2006 eruptive period, inferred from remote spectroscopic measurements of SO₂ emissions. *J. Volcanol. Geother. Res.*, 176, pp. 151-162.
- Ball, M. & Pinkerton, H. (2006). Factors controlling the accuracy of thermal imaging cameras. *J. Geophys. Res.*, 111, B11203, doi: 10.1029/2005JB003829.
- Ball, M., Pinkerton, H. & Harris, A.J.L. (2008). Surface cooling, advection and the development of different surface textures on active lavas on Kilauea, Hawai'i. *J. Volcanol. Geotherm. Res.*, 173, pp. 148-156.
- Bluth, G.J.S., Shannon, J.M., Watson, I.M., Prata, A.J. & Realmuto, V.J. (2007). Development of an ultra-violet digital camera for volcanic SO₂ imaging. *J. Volcanol. Geotherm. Res.*, 161, pp. 47-56.
- Bobrowski, N., Hönninger, G., Galle, B. & Platt, U. (2003). Detection of bromine monoxide in a volcanic plume. *Nature*, 423, pp. 273-276.
- Branan, Y.K., Harris, A., Watson, I.M., Phillips, J.C., Horton, K., Williams-Jones, G. & Garbeil, H. (2008). Investigation of at-vent dynamics and dilution using thermal infrared radiometers at Masaya volcano, Nicaragua. *J. Volcanol. Geotherm. Res.*, 169, pp. 34-47.
- Burton, M.R., Oppenheimer, C., Horrocks, L.A. & Francis, P.W. (2000). Remote sensing of CO₂ and H₂O emission rates from Masaya volcano, Nicaragua. *Geology*, 28, pp. 915-918.
- Burton, M.R., Oppenheimer, C., Horrocks, L.A. & Francis, P.W. (2001). Diurnal changes in volcanic plume chemistry observed by lunar and solar occultation spectroscopy. *Geophys. Res. Lett.*, 28(5), pp. 843-846.
- Caltabiano, T., Romano, R. & Budetta, G. (1994). SO₂ flux measurements at Mount Etna, Sicily. *J. Geophys. Res.*, 99(D6), pp. 12,809-12,819.
- Calvari, S., Spampinato, L., Lodato, L., Harris, A.J.L., Patrick, M., Dehn, J., Burton, M.R. & Andronico, D. (2005). Chronology and complex volcanic processes during the 2002-2003 flank eruption at Stromboli volcano (Italy) reconstructed from direct observations and surveys with a handheld thermal camera. *J. Geophys. Res.*, 110, B02201, doi:10.1029/2004JB003129.
- Calvari, S., Spampinato, L. & Lodato, L. (2006). The 5 April 2003 vulcanian paroxysmal explosion at Stromboli volcano (Italy) from field observations and thermal data. *J. Volcanol. Geotherm. Res.*, 149, pp. 160-175.
- Calvari, S., Lodato, L., Steffke, A., Cristaldi, A., Harris, A.J.L., Spampinato, L. & Boschi, E. (2010). The 2007 Stromboli eruption: Event chronology and effusion rates using thermal infrared data. *J. Geophys. Res.*, 115, B04201, doi:10.1029/2009JB006478.

- Carn, S.A., Krueger, A.J., Bluth, G.J.S., Schaefer, S.J., Krotkov, N.A., Watson, I.M. & Datta, S. (2003). Volcanic eruption detection by the Total Ozone Mapping Spectrometer (TOMS) instruments: a 22-year record of sulfur dioxide and ash emissions. In: Oppenheimer, C., Pyle, D.M. & Barclay, J. (Eds.), *Volcanic Degassing*. Geological Society, London, Sp. Pub., 213, pp. 177-202.
- Carroll, M.R. & Holloway, J.R. (1994). Volatiles in magmas: Mineralogical Society of America *Reviews in Mineralogy*, vol. 30.
- Carroll, M.R. & Webster, J.D. (1994). Solubilities of sulfur, noble gases, nitrogen, chlorine and fluorine in magmas. In: Carroll, M.R., Holloway, J.R. (Eds.), *Volatiles in Magmas, Rev. in Mineralogy*, vol. 30, pp. 231-279.
- Casadevall, T.J., Johnston, D.A., Harris, D.M., Rose, W.I., Malinconico, L.L., Stoiber, R.E., Bornhorst, T.J., Williams, S.N., Woodruff, L. & Thompson, J.M. (1981). SO₂ emission rates at Mount St. Helens from March 29 through December, 1980. In: Lipman, P.W. & Mullineaux, D.L. (Eds.), *The 1980 eruptions of Mount St. Helens, Washington. U.S. Geol. Surv., Prof. Pap.*, vol. 1250, pp. 193-200.
- Chance, K. (1998). Analysis of BrO measurements from the global ozone monitoring experiment. *Geophys. Res. Lett.*, 25, pp. 3335-3338.
- Corsaro, R.A. & Miraglia, L. (2005). Dynamics of 2004-2005 Mt. Etna effusive eruption as inferred from petrologic monitoring. *Geophys. Res. Lett.*, 32, L13302, doi:10.1029/2005GL022347.
- Daag, A.S., Tubianosa, B.S. et al. (1996). Monitoring sulphur dioxide emission at Mount Pinatubo. In: Newhall, C.G. & Punongbayan, R.S. (Eds.), *Fire and mud: eruptions and lahars of Mount Pinatubo Philippines*, *Philippine Institute of Volcanology and Seismology, Quezon City, University of Washington Press*, Seattle, pp. 409-434.
- Dean, K.G., Dehn, J., Papp, K.R., Smith, S., Izbekov, P., Peterson, R., Kearney, C. & Steffke, A. (2004). Integrated satellite observations of the 2001 eruption of Mt. Cleveland, Alaska. *J. Volcanol. Geotherm. Res.*, 135, pp. 51-73.
- Dehn, J., Dean, K.G., Engle, K. & Izbekov, P. (2002). Thermal precursors in satellite images of the 1999 eruption of Shishaldin Volcano. *Bull. Volcanol.*, 64(8), pp. 525-534.
- Delgado-Granados, H., Cárdenas González, L. & Piedad Sánchez, N. (2001). Sulfur dioxide emissions from Popocatepetl volcano (Mexico): case study of a high-emission rate, passively degassing erupting volcano. *J. Volcanol. Geotherm. Res.*, 108, pp. 107-120.
- Delmelle, P., Baxter, P., Baulieu, A., Burton, M., Francis, P., Garcia-Alvarez, J., Horrocks, L., Navarro, M., Oppenheimer, C., Rothery, D., Rymer, H., St-Amand, K., Stix, J., Strauch, W. & Williams-Jones, G. (1999). Origin, effects of Masaya volcano's continued unrest probed in Nicaragua. *EOS, Transactions, Am. Geophys. Union*, 80, pp. 575-581.
- Delmelle, P., Stix, J., Baxter, P.J., Garcia-Alvarez, J. & Barquero, J. (2002). Atmospheric dispersion, environmental effects and potential health hazard associated with the low-altitude gas plume of Masaya volcano, Nicaragua. *Bull. Volcanol.*, 64, pp. 423-434.
- Doukas, M.P. (2002). A new method for GPS-based wind speed determinations during airborne volcanic plume measurements. *U.S. Geol. Surv., Open-File Rep.* 02-395, pp. 1-13.
- Duffell, H.J., Oppenheimer, C., Pyle, D.M., Galle, B., McGonigle, A.J.S. & Burton, M.R. (2003). Changes in gas composition prior to a minor explosive eruption at Masaya volcano, Nicaragua. *J. Volcanol. Geotherm. Res.*, 126, pp. 327-339.

- Edmonds, M., Herd, R.A., Galle, B. & Oppenheimer, C. (2003). Automated, high time-resolution measurements of SO₂ flux at Soufrière Hills Volcano, Montserrat, West Indies. *Bull. Volcanol.*, 65, pp. 578-586.
- Edmonds, M. (2008). New geochemical insights into volcanic degassing. *Phil. Trans. R. Soc.*, 366, pp. 4559-4579.
- Fayt, C. & van Roozendael, M. (2001). WinDOAS 2.1-Software User Manual. Belgisch Instituut voor Ruimte-Aeronomie Institut D'Aéronomie Spatiale de Belgique, Brussels, Belgium.
- Finnegan, D.L., Kotra, J.P., Hermann, D.M. & Zoeller, W.H. (1989). The use of 7LiOH-impregnated filters for the collection of acidic gases and analysis by instrumental neutron activation analysis. *Bull. Volcanol.*, 51, pp. 83-87.
- Fish, D.J. & Jones, R.L. (1995). Rotational Raman scattering and the ring effect in zenith-sky spectra. *Geophys. Res. Lett.*, 22(7), pp. 811-814.
- Galle, B., Oppenheimer, C.M., Geyer, A., McGonigle, A. & Edmonds, M. (2003). A mini-DOAS spectrometer applied in remote sensing of volcanic SO₂ emissions. *J. Volcanol. Geotherm. Res.*, 119, pp. 241-254.
- Galle, B., Johansson, M., Rivera, C., Zhang, Y., Kihlman, M., Kern, C., Lehmann, T., Platt, U., Arellano, S. & Hidalgo, S. (2010). Network for Observation of Volcanic and Atmospheric Change (NOVAC) A global network for volcanic gas monitoring: Network layout and instrument description. *J. Geophys. Res.*, 115, D05304, doi:10.1029/2009JD011823.
- Giberti, G., Jaupart, C. & Sartoris, G. (1992). Steady-state operation of Stromboli volcano, Italy: Constraints on the feeding system. *Bull. Volcanol.*, 54, pp. 535-541.
- Giggenbach, W.F. (1996). Chemical composition of volcanic gases. In: Scarpa, R., Tilling, R.I. (Eds.), Monitoring and mitigation of volcanic hazards, Berlin-Heidelberg, Springer Verlag, pp. 221-256.
- Giggenbach, W.F. & Goguel, R.L. (1989). Collection and analysis of geothermal and volcanic water and gas discharges. *Department of Scientific and Industrial Research, New Zealand*, report CD2401, 81.
- Gilbert, J.S. & Sparks, R.S.J. (1998). The Physics of Explosive Volcanic Eruptions. *Geol. Soc. Sp. Pub.*, vol. 145.
- Hamilton, P.M., Varey, R.H. & Millán, M.M. (1978). Remote sensing of sulphur dioxide. *Atmospheric Envir.*, 12, pp. 127-133.
- Harris, A.J.L., Flynn, L.P., Rothery, D.A., Oppenheimer, C. & Sherman, S.B. (1999). Max flux measurements at active lava lakes: Implications for magma recycling. *J. Geophys. Res.*, 104, pp. 7117-7136.
- Harris, A.J.L. (2009). The pit-craters and pit-crater-filling lavas of Masaya volcano. *Bull. Volcanol.*, 71, pp. 541-558.
- Harris, A.J.L., Steffke, A., Calvari, S. & Spampinato, L. (2011). Thirty years of satellite-derived lava discharge rates at Etna: Implications for steady volumetric output. *J. Geophys. Res.*, 116, B08204, doi:10.1029/2011JB008237.
- Horrocks, L.A., Burton, M., Francis, P. & Oppenheimer, C. (1999). Stable gas plume composition measured by OP-FTIR spectroscopy at Masaya volcano, Nicaragua, 1998-1999. *Geophys. Res. Lett.*, 26, pp. 3497-3500.
- Horrocks, L.A. (2001). Infrared spectroscopy of volcanic gases at Masaya, Nicaragua. *PhD thesis*, Open University, UK.

- Horrocks, L.A., Oppenheimer, C., Burton, M.R. & Duffell, H.J. (2003). Compositional variation in tropospheric volcanic gas plumes: evidence from ground-based remote sensing. In: Oppenheimer, C., Pyle, D.M. & Barclay, J. (Eds.), *Volcanic Degassing*, Geological Society, London. 149-168. ISBN: 978-1-86239-136-9.
- Horton, K.A., Williams-Jones, G., Garbeil, H., Elias, T., Sutton, A.J., Mouginiis-Mark, P., Porter, J.N. & Clegg, S. (2006). Real-time measurement of volcanic SO₂ emissions: validation of a new UV correlation spectrometer (FLYSPEC). *Bull. Volcanol.*, 68, pp. 323-327.
- Huppert, H.E. & Woods, A.W. (2002). The role of volatiles in magma chamber dynamics. *Nature*, vol. 420, pp. 493-495.
- Kern, C. (2009). Spectroscopic measurements of volcanic gas emissions in the ultra-violet wavelength region. *Ph.D. thesis*, Univ. of Heidelberg, Heidelberg, Germany.
- Kern, C., Sihler, H., Vogel, L., Rivera, C., Herrera, M. & Platt, U. (2009a). Halogen oxide measurements at Masaya Volcano, Nicaragua using active path differential optical absorption spectroscopy. *Bull. Volcanol.*, 71, pp. 659-670.
- Kern, C., Deutschmann, T., Vogel, A., Wöhrbach, M., Wagner, T., & Platt, U. (2009b). Radiative transfer corrections for accurate spectroscopic measurements of volcanic gas emissions, *Bull. Volcanol.*, doi:10.1007/s00445-009-0313-7.
- Keszthelyi, L. & Denlinger, R. (1996). The initial cooling of pahoehoe flow lobes. *Bull. Volcanol.*, 58, pp. 5-18.
- Keszthelyi, L., Harris, A.J.L. & Dehn, J. (2003). Observations of the effect of wind on the cooling of active lava flows. *Geophys. Res. Lett.*, 30(19), doi:10.1029/2003GL017994.
- Kyle, P.R., Sybelton, L.M., McIntosh, W.C., Meeker, K. & Symonds, R. (1994). Sulfur dioxide emission rates from Mount Erebus, Antarctica. In: Kyle, P. (Ed.), *Volcanological and environmental studies of Mount Erebus, Antarctica*, Washington D.C., AGU, *Antarctic Research Series*, vol. 66, pp. 69-82.
- Lodato, L., Spampinato, L., Harris, A.J.L., Calvari, S., Dehn, J. & Patrick, M. (2007). The morphology and evolution of the Stromboli 2002-2003 lava flow field: An example of basaltic flow field emplaced on a steep slope. *Bull. Volcanol.*, 69, pp. 661-679.
- Malicet, J., Daumont, D., Charbonnier, J., Parisse, C., Chakir, A. & Brion, J. (1995). Ozone UV spectroscopy. II. Absorption cross-sections and temperature dependence. *J. Atmos. Chem.*, 21, pp. 263. doi:10.1007/BF00696757.
- Malinconico, L.L. (1979). Fluctuations in SO₂ emission during recent eruptions of Etna. *Nature*, 278, pp. 43-45.
- Manatt, S.L. & Lane, A.L. (1993). A compilation of the absorption cross-section of SO₂ from 106 to 403 nm. *J. Quant. Spectrosc. Radiat. Transfer.*, 50(3), pp. 267-276.
- Martin, R.S., Mather, T.A., Pyle, D.M., Power, M., Tsanev, V.I., Oppenheimer, C., Allen, A.G., Horwell, C.J. & Ward, E.P.W. (2009). Size distributions of fine silicate and other particles in Masaya's volcanic plume. *J. Geophys. Res.*, 114, D09217.
- Martin, R.S., Sawyer, G.M., Spampinato, L., Salerno, G.G., Ramirez, C., Ilyinskaya, E., Witt, M.L.I., Mather, T.A., Watson, I.M., Phillips, J.C. & Oppenheimer, C. (2010). A total volatile inventory for Masaya Volcano, Nicaragua. *J. Geophys. Res.*, 115, B09215, doi: 10.1029/2010JB007480.
- Mather, T.A., Allen, A.G., Oppenheimer, C., Pyle, D.M. & McGonigle, A.J.S. (2003). Size-resolved characterisation of soluble ions in the particles in the tropospheric plume

- of Masaya volcano, Nicaragua: origins and plume processing. *J. Atmosph. Chem.*, 46, pp. 207-237.
- Mather, T.A., Pyle, D.M., Tsanev, V.I., McGonigle, A.J.S., Oppenheimer, C., & Allen, A.G. (2006). A reassessment of current volcanic emissions from the Central American arc with specific examples from Nicaragua. *J. Volcanol. Geotherm. Res.*, 149, pp. 297-311
- McBirney, A.R. (1956). The Nicaraguan volcano Masaya and its caldera. *Trans. Amer. Geophys. Union*, 37, pp. 83-96.
- McGee, K.A. & Sutton, J.A. (1994). Eruptive activity at Mount St Helens, Washington, USA, 1984-1988: a gas geochemistry perspective. *Bull. Volcanol.*, 56, pp. 435-446.
- McGonigle, A.J.S. & Oppenheimer, C. (2003). Optical sensing of volcanic gas and aerosol emissions. In: Oppenheimer, C., Pyle, D.M. & Barclay, J. (Eds.), *Volcanic Degassing*, Geological Society, London. 149-168. ISBN: 978-1-86239-136-9.
- McGonigle, A.J.S., Oppenheimer, C., Hayes, A.R., Galle, B., Edmonds, M., Caltabiano, T., Salerno, G., Burton, M. & Mather, T.A. (2003). Sulphur dioxide fluxes from Mt. Etna, Vulcano and Stromboli measured with an automated scanning ultraviolet spectrometer. *J. Geophys. Res.*, 108(B9), 2455. doi:10.1029/2002JB002261.
- McGonigle, A.J.S., Delmelle, P., Oppenheimer, C., Tsanev, V.I., Delfosse, T., Williams-Jones, G., Horton, K. & Mather, T.A. (2004). SO₂ depletion in tropospheric volcanic plumes. *Geophys. Res. Lett.*, 31, L13201, doi: 10.1029/2004GL019990.
- McGonigle, A.J.S., Aiuppa, A., Ripepe, M., Kantzas, E.P. & Tamburello, G. (2009). Spectroscopic capture of 1 Hz volcanic SO₂ fluxes and integration with volcano geophysical data. *Geophys. Res. Lett.*, 36, L21309, doi:10.1029/2009gl040494.
- Millan, M.M. (1980). Remote sensing of air pollutants. A study of some atmospheric scattering effects. *Atmos. Env.*, 14, pp. 1241-1253.
- Mouginis-Mark, P.J., Crisp, J.A. & Fink, J.H. (2000). In: Mouginis-Mark, P.J., Crisp, J.A. & Fink, J.H. (Eds.), *Remote Sensing of Active Volcanism*, AGU, *Geophysical Monograph*, 116, pp. 1-7.
- Nadeau, P. & Williams-Jones, G. (2009). Apparent downwind depletion of volcanic SO₂ flux-lessons from Masaya Volcano, Nicaragua. *Bull. Volcanol.*, 71, pp. 389-400.
- Neri, A. (1989). A local heat transfer analysis of lava cooling in the atmosphere: application to thermal diffusion-dominated lava flows. *J. Volcanol. Geotherm. Res.*, 81, pp. 215-243.
- Newcomb, G. & Millán, M.M. (1970). Theory, applications and results of the long-line correlation spectrometer. *IEEE Trans. Geosci. Electron.*, 8, pp. 149-157.
- Noguchi, K. & Kamiya, H. (1963). Prediction of volcanic eruption by measuring the chemical composition and amounts of gases. *Bull. Volcanol.*, 26, pp. 367-378.
- Noxon, J.F. (1975). Nitrogen dioxide in stratosphere and troposphere measured by round-based absorption spectroscopy. *Science*, 189, pp. 547-549.
- O'Dwyer, M., McGonigle, A.J.S., Padgett, M.J., Oppenheimer, C. & Inguaggiato, S. (2003). Real time measurements of volcanic H₂S/SO₂ ratios by UV spectroscopy. *Geophys. Res. Lett.*, 30, 12, doi:10.1029/2003GL017246.
- Olmos, R., Barrancos, J., Rivera, C., Barahona, F., López, D.L., Henriquez, B., Hernández, A., Benitez, E., Hernández, P.A., Pérez, N.M. & Galle, B. (2007). Anomalous emissions of SO₂ during the recent eruption of Santa Ana Volcano, El Salvador, Central America. *Pure Appl. Geophys.*, 164, pp. 2489-2506.
- Oppenheimer, C. & Francis, P. (1997). Remote sensing of heat, lava and fumarole emissions from Erta 'Ale volcano, Ethiopia. *Int. J. Remote Sens.*, 18(8), pp. 1661-1692.

- Oppenheimer, C., Francis, P., & Stix J. (1998). Depletion rates of sulphur dioxide in tropospheric volcanic plumes. *Geophys. Res. Lett.*, 25(14), pp. 2671-2674.
- Oppenheimer, C. (2003). Volcanic degassing. In: Rudnick, R.L., Holland, H.D., Turekian, K.K. (Eds.), *The crust, Treatise on geochemistry, Oxford, Elsevier-Pergamon*, vol. 3, pp. 123-166.
- Oppenheimer, C., McGonigle, A.J.S., Allard, P., Wooster, M.J. & Tsanev, V. (2004). Sulfur, heat, and magma budget of Erta 'Ale lava lake, Ethiopia. *Geology*, 32(6), 509-512.
- Oppenheimer, C., Kyle, P.R., Tsanev, V.I., McGonigle, A.J.S., Mather, T.A. & Sweeney, D. (2005). Mt. Erebus, the largest point source of NO₂ in Antarctica. *Atmos. Environ.*, 39, pp. 6000-6006.
- Perez, M., Freundt, A., Kutterolf, S. & Schminke, H.-U. (2009). The Masaya triple layer: A 2100 year old basaltic multiepisodic Plinian eruption from the Masaya Caldera Complex (Nicaragua). *J. Volcanol. Geotherm. Res.*, 179(3-4), pp. 191-205.
- Platt, U. (1994). Differential optical absorption spectroscopy (DOAS). In: Sigrist, M.W. (Ed.), *Air monitoring by spectroscopic techniques, Chemical Analysis Series*, vol. 127, Wiley, J., Chichester, UK.
- Platt, U. & Stutz, J. (2008). *Differential Optical Absorption Spectroscopy principles and applications, Series: Physics of Earth and Space Environment*, Springer.
- Rausch, J. & Schminke, H.-U. (2010). Nejapa Tephra: The youngest (c. 1 ka BP) highly explosive hydroclastic eruption in western Managua (Nicaragua). *J. Volcanol. Geotherm. Res.*, 192, pp. 159-177.
- Realmuto, V.J. (2000). The potential use of earth observing system data to monitor the passive emission of sulfur dioxide from volcanoes. In: Mouginis-Mark, P.J., Crisp, J.A. & Fink, J.H. (Eds.), *Remote sensing of active volcanism, Geophys. Monogr. AGU*, Washington, D.C., vol. 116, pp. 101-115.
- Roche, O., van Wyk de Vries, B. & Druitt, T.H. (2001). Sub-surface structures and collapse mechanisms of summit pit craters. *J. Volcanol. Geotherm. Res.*, 105, pp. 1-18.
- Rodríguez, L.A., Branan, Y.K., Watson, I.M., Bluth, G.J.S., Rose, W.I., Chigna, G., Matías, O., Carn, S.A. & Fischer, T. (2004). SO₂ emissions to the atmosphere from active volcanoes in Guatemala and El Salvador, 1999-2002. *J. Volcanol. Geotherm. Res.*, 138, pp. 325-344.
- Rymer, H., van Wyk de Vries, B., Stix, J. & Williams-Jones, G. (1998). Pit crater structure and processes governing persistent activity at Masaya volcano, Nicaragua. *Bull. Volcanol.*, 59, pp. 345-355.
- Salerno, G.G., Burton, M.R., Oppenheimer, C., Caltabiano, T., Randazzo, D., Bruno, N. & Longo, V. (2009a). Three-years of SO₂ flux measurements of Mt. Etna using an automated UV scanner array: Comparison with conventional traverses and uncertainties in flux retrieval. *J. Volcanol. Geotherm. Res.*, 183, pp. 76-83.
- Salerno, G.G., Burton, M.R., Oppenheimer, C., Caltabiano, T., Tsanev, V.I. & Bruno, N. (2009b). Novel retrieval of volcanic SO₂ abundance from ultraviolet spectra. *J. Volcanol. Geotherm. Res.*, 181, pp. 141-153.
- Solomon, S., Schmeltekopf, A.L. & Sanders, R.W. (1987). On the interpretation of zenith sky absorption measurements. *J. Geophys. Res.*, 92, pp. 8311-319.
- Spampinato, L., Calvari, S., Oppenheimer, C. & Lodato, L. (2008a). Shallow magma transport for the 2002-3 Mt. Etna eruption inferred from thermal infrared surveys. *J. Volcanol. Geotherm. Res.*, 177, pp. 301-312.

- Spampinato, L., Oppenheimer, C., Calvari, S., Cannata, A. & Montalto, P. (2008b). Lava lake surface characterization by thermal imaging: Erta 'Ale volcano (Ethiopia). *Geochem. Geophys. Geosyst.*, 9, Q12008. doi:10.1029/2008GC002164.
- Spampinato, L., Calvari, S., Oppenheimer, C. & Boschi, E. (2011). Volcano surveillance using infrared cameras. *Earth Sci. Rev.*, 106, pp. 63-91.
- Sparks, R.S.J. (2003). Dynamics of magma degassing. In: Oppenheimer, C., Pyle, D.M., Barclay, J. (Eds.), *Volcanic degassing*, *Geol. Soc. Lond., Sp. Pub.*, vol. 213, pp. 5-22.
- Spilliaert, N., Allard, P., Metrich, N. & Sobolev, A.V. (2006). Melt inclusion record of the conditions of ascent, degassing, and extrusion of volatile-rich alkali basalt during the powerful 2002 flank eruption of Mount Etna (Italy). *J. Geophys. Res.*, 111, B04203, doi:10.1029/2005jb003934.
- Steffke, A.M., Harris, A.J.L., Burton, M., Caltabiano, T. & Salerno G.G. (2010). Coupled use of COSPEC and satellite measurements to define the volumetric balance during effusive eruptions at Mt. Etna, Italy. *J. Volcanol. Geotherm. Res.*, 205, pp. 47-53.
- Stix, J. (2007). Stability and instability of quiescently degassing active volcanoes: The case of Masaya, Nicaragua. *Geology*, 35(6), pp. 535-538.
- Stoiber, R.E. & Jepsen, A. (1973). Sulphur dioxide contribution to the atmosphere by volcanoes. *Science*, 182, pp. 577-578.
- Stoiber, R.E., Malinconico, L.L. & Williams, S.N. (1983). Use of the correlation spectrometer at volcanoes. In: Tazieff, H. & Sabroux, J.-C. (Eds.), *Forecasting volcanic events*, *Elsevier*, Amsterdam, pp. 425-444.
- Stoiber, R., Williams, S. & Huebert, B. (1986). Sulfur and halogen gases at Masaya caldera complex, Nicaragua: total flux and variations with time, *J. Geophys. Res.*, 91(B12), pp. 12,215-12,231.
- Sutton, A.J., Elias, T., Gerlach, T.M. & Stokes, J.B. (2001). Implications for eruptive processes as indicated by sulfur dioxide emissions from Kilauea Volcano, Hawai'i, 1979-1997. *J. Volcanol. Geotherm. Res.*, 108(1-4), pp. 283-302.
- Symonds, R.B., Rose, W.I., Bluth, G.J.S. & Gerlach, T.M. (1994). Volcanic gas studies methods, results, and applications. *Rev. Mineral.*, 30, pp. 1-66.
- Symonds, R.B., Gerlach, T.M. & Reed, M.H. (2011). Magmatic gas scrubbing: implications for Volcano monitoring. *J. Volcanol. Geothermal Res.*, 108, pp. 303-341.
- Sweeney, D., Kyle, P.R. & Oppenheimer C. (2008). Sulfur dioxide emissions and degassing behavior of Erebus volcano, Antarctica. *J. Volcanol. Geother. Res.*, 177(3), pp. 725-733.
- Thomas, H.E. & Watson, I.M. (2010). Observations of volcanic emissions from space: current and future perspectives. *Nat. Hazards*, 54, pp. 323-354.
- Tilling, R.I. (1987). Fluctuations in surface height of active lava lakes during 1972-1974 Mauna Ulu eruption, Kilauea volcano, Hawai'i. *J. Geophys. Res.*, 92, 13721-13730.
- Torrence, C. & Compo, G.P. (1998). A practical guide to wavelet analysis. *Bull. Am. Meteorol. Soc.*, 79, pp. 61-78.
- Vandaele, A.C., Simon, P.C., Guilmoit, J.M., Carleer, M. & Colin, R. (1994). SO₂ absorption cross section measurement in the UV using a Fourier transform spectrometer. *J. Geophys. Res.*, 99, pp. 25,599-25,605.
- Vicari, A., Ciraudó, A., Del Negro, C., Herault, A. & Fortuna, L. (2008). Lava flow simulations using discharge rates from thermal infrared satellite imagery during the 2006 Etna eruption. *Nat. Hazards*, doi:10.1007/s11069-008-9306-7.

- Villemant, B. & Boudon, G. (1999). H₂O and halogen (F, Cl, Br) behavior during shallow magma degassing processes. *Earth Planet. Sci. Lett.*, 168, pp. 271-286.
- Wallace, P.J. & Gerlach, T.M. (1994). Magmatic vapour source for sulphur dioxide released during volcanic eruptions: evidence from Mount Pinatubo. *Science*, 265, pp. 497-499.
- Wardell, L.J., Kyle, P.R. & Campbell, A.R. (2003). Carbon dioxide emissions from fumarolic ice towers, Mount Erebus volcano, Antarctica. In: Oppenheimer, C., Pyle, D.M. & Barclay, J. (Eds.), *Volcanic degassing, Geol. Soc. Lond., Sp. Pap.*, vol. 213, pp. 231-246.
- Williams, S.N. (1983). Geology and eruptive mechanisms of Masaya caldera complex. *PhD thesis*, Dartmouth College, Hanover, N.H..
- Williams-Jones, G. (2001). Integrated geophysical studies at Masaya volcano, Nicaragua, *Ph.D. thesis*, Open Univ., UK.
- Williams-Jones, G., Rymer, H. & Rothery, D.A. (2003). Gravity changes and passive SO₂ degassing at the Masaya caldera complex, Nicaragua. *J. Volcanol. Geotherm. Res.*, 123(1-2), pp. 37-160.
- Williams-Jones, G., Stix, J. & Hickson, C. (2008). The COSPEC Cookbook: making SO₂ measurements at active volcanoes. IAVCEI, *Methods in Volcanology*, vol. 1.
- Witham, F., Woods, A.W. & Gladstone, C. (2006). An analogue experimental model of depth fluctuations in lava lakes. *Bull. Volcanol.*, 69, pp. 51-56.
- Witt, M.L.I., Mather, T.A., Pyle, D.M., Aiuppa, S., Bagnato, E. & Tsanev, V.I. (2008). Mercury and halogens emissions from Masaya and Telica volcanoes, Nicaragua. *J. Geophys. Res.*, 113, B06203, doi: 10.1029/2007JB005401.
- Wright, R. & Pilger, E. (2008). Satellite observations reveal little inter-annual variability in the radiant flux from the Mount Erebus lava lake. *J. Volcanol. Geotherm. Res.*, 177, pp. 687-694.
- Wright, R., Garbeil, H. & Davies, A.G. (2010). Cooling rate of some active lavas determined using an orbital imaging spectrometer. *J. Geophys. Res.*, 115, B06205, doi:10.1029/2009JB006536.
- Young, S.R., Sparks, R.S.J., Aspinall, W.P., Lynch, L.L., Miller, A.D., Robertson, R.E.A. & Shepherd, J.B. (1998). Overview of the eruption of Soufriere Hills volcano, Montserrat, 18 July 1995 to December 1997. *Geophys. Res. Lett.*, 25(18), pp. 3389-3392.
- Zapata, J.A., Calvache, M.L. et al. (1997). SO₂ fluxes from Galeras Volcano, Colombia, 1989-1995: Progressive degassing and conduit obstruction of a Decade Volcano. *J. Volcanol. Geotherm. Res.*, 77, pp. 195-208.